
The Subjectivity of Monoculture

Nathanael Jo¹ Nikhil Garg² Manish Raghavan¹

Abstract

Machine learning models – including large language models (LLMs) – are often said to exhibit *monoculture*, where outputs agree strikingly often. But what does it actually mean for models to agree too much? We argue that this question is inherently subjective, relying on two key decisions.

First, the analyst must specify a baseline null model for what “independence” should look like. This choice is inherently subjective, and as we show, different null models result in dramatically different inferences about excess agreement. Second, we show that inferences depend on the population of models and items under consideration. Models that seem highly correlated in one context may appear independent when evaluated on a different set of questions, or against a different set of peers. Experiments on two large-scale benchmarks validate our theoretical findings. For example, we find drastically different inferences when using a null model with item difficulty compared to previous works that do not. Together, our results reframe monoculture evaluation not as an absolute property of model behavior, but as a context-dependent inference problem.

1. Introduction

A growing body of empirical work suggests that AI models, including both predictive and generative models, produce homogeneous outputs. Across domains – including text/image generation, factual responses, and decision making – separately trained models often produce strikingly similar responses (Wu et al., 2025; Padmakumar & He, 2024; Raghavan, 2024; Ugander & Epstein, 2024; Doshi & Hauser, 2024; Goel et al., 2025; Kim et al., 2025; Toups et al., 2023; Wenger & Kenett, 2025). Throughout the literature, a common perspective has emerged: Models don’t just agree, they agree *too much*, resulting in “algorithmic monoculture” (Kleinberg & Raghavan, 2021).

¹MIT, Cambridge, USA ²Cornell Tech, New York, USA. Correspondence to: Nathanael Jo <nathanjo@mit.edu>.

Preprint. March 2, 2026.

Why does monoculture matter? In resource allocation settings such as hiring or lending, similar predictive systems may lead institutions to systematically privilege or disadvantage the same groups (Jain et al., 2024). In market settings, firms that independently deploy similar pricing algorithms may inadvertently sustain higher prices and harm consumers (Jo et al., 2025). More broadly, diversity is often a desirable property of sociotechnical systems because it can improve robustness to error, reflect a plurality of norms or preferences, and promote creative or novel outputs. A large literature has emerged analyzing the downstream consequences of algorithmic monoculture (Bommasani et al., 2022; Creel & Hellman, 2022; Peng & Garg, 2024a,b; Baek et al., 2025).

However, claims about monoculture are by nature relative, because it suggests that outputs are more correlated than one would expect under some ideal world. As we will show, this comparison cannot be made in a vacuum. Instead, it requires two subjective choices made by the analyst, and these choices drive the conclusions they reach about monoculture:

1. What is the baseline (null model) against which agreement is measured?
2. On what population of models and instances do we measure excess agreement?

Baselines for excess agreement. The literature contains two distinct approaches to constructing baselines against which excess agreement is measured. One is to use human subjects (Wu et al., 2025; Padmakumar & He, 2024; Ugander & Epstein, 2024; Doshi & Hauser, 2024; Anderson et al., 2024). While human baselines are useful for normative comparisons about diversity, they require committing to a reference population and a notion of human diversity.

A second approach, and one we take here, is to measure excess agreement relative to a “null model,” under which responses are conditionally independent (Kim et al., 2025; Gorecki & Hardt, 2025; Goel et al., 2025; Toups et al., 2023). A null model is a particular data-generating process that creates an expectation of how much agreement is reasonable. Any observed agreement in excess of the null model is potentially evidence of monoculture. A popular null model is capability-based (Goel et al., 2025; Jo et al., 2025). In its simplest form, two models with accuracies (p_1, p_2) are viewed as independent if their expected agreement is the

chance overlap p_1p_2 on each item.

Is this the “right” null model? Perhaps—but this baseline might ignore other relevant features. For example, questions may vary in difficulty: if two models both succeed on easy items and fail on hard ones, their agreement may substantially exceed the p_1p_2 baseline even in the absence of any meaningful dependence. Or perhaps some models perform well on math questions, whereas others excel at writing code. Again, this would lead to excess agreement beyond what the simple p_1p_2 baseline would predict. More generally, a null model allows us to express structure in our observations that we *expect* to see, giving us a baseline against which to measure *unexpected* correlation.

Complicating things further is that we generally lack “ground truth” information about latent structural properties like item difficulty. Instead, we must infer them from data: e.g., the difficult questions are precisely the ones that many models get wrong. With a small set of models, one might incorrectly attribute all correlation to heterogeneous item difficulty, thereby failing to detect any excess correlation. In other words, latent structural properties like item difficulty or model capability cannot be defined in a context-free way; they are defined only relative to a population of models and items. As a result, even after fixing a null model, conclusions about excess agreement depend critically on the set of models and questions over which it is fit and evaluated.

Our contributions. We begin in Section 2 by arguing that claims of monoculture are best understood as *comparative analyses*. Under this view, monoculture is not an absolute property of a dataset, but a discrepancy between observed behavior and a researcher-chosen baseline.

In Section 3, we show that the choice of null model is inherently subjective. Different reasonable assumptions about some latent structure give rise to different notions of independence—and hence different conclusions about excess correlation. Therefore, one must select and defend a reasonable null model grounded on priors and available data. We empirically demonstrate our theoretical findings using two large multi-choice benchmarks. In particular, we find drastically different inferences when using a null model with item difficulty compared to previous works that do not.

Finally, in Section 4, we show that even after fixing a null model, inference is sensitive to the population of models and items included in the analysis. For example, when the models are highly homogeneous, it may be difficult to isolate true correlation beyond what the null might explain.

Together, these results clarify that monoculture claims are jointly shaped by the choice of null model *and* the evaluative context in which it is fit. We discuss the implications of our work for future research and analysis in Section 5. We also provide an extended related work in Appendix A.

2. The Null Model of Independence

In this section, we formalize what it means to assess monoculture relative to an independent baseline. We study a setting in which models answer n independent items, and we ask whether the observed data can be explained by “independent” model behavior. To do so, we introduce a *null model of independence*: a family of joint distributions in which all dependence arises through latent parameters.

2.1. Setup

We observe, for each item $i \in \{1, \dots, n\}$ and each model $j \in \{1, \dots, m\}$, an output Y_{ij} with values in an output space \mathcal{Y} , taken from some unknown probability distribution P . Throughout the paper, we instantiate our theory in the simplest setting, $\mathcal{Y} = \{0, 1\}$, where Y_{ij} encodes correctness. This choice allows us to highlight the core identification issues without additional complexity, as well as reflecting the paradigm others have studied.¹ We show how to generalize our framework to other output spaces in Appendix D.1.

2.2. Monoculture with respect to a null

We argue that claims of “monoculture” are only meaningful relative to a chosen *null model* of independence. In the binary setting $\mathcal{Y} = \{0, 1\}$, each model output Y_{ij} is a Bernoulli random variable. Let Θ be an arbitrary parameter space encoding such latent factors (e.g., item properties, model abilities, or both). For each $\theta \in \Theta$, define a *product-Bernoulli model* on $\{0, 1\}^m$ by

$$P_\theta(y_1, \dots, y_m) := \prod_{j=1}^m p_{\theta_j}^{y_j} (1 - p_{\theta_j})^{1-y_j},$$

where each $p_{\theta_j} \in [0, 1]$ is the conditional success probability of model j under parameter θ . A null model is the family of distributions $\mathcal{P}_{\text{null}} := \{P_\theta : \theta \in \Theta\}$, and a joint law P is consistent with the null model if it lies in this set. In other words, under the null model, all inter-model agreement can be explained by the shared latent parameter θ together with **conditional independence across models**.

3. Subjectivity of Null Model

In general, there are numerous choices of Θ , many of which are “reasonable” null models. As in the example in Section 1, a simpler null model that only accounts for accuracy might imply a higher observed correlation than if we additionally included item difficulties. In other words, expanding Θ enlarges $\mathcal{P}_{\text{null}}$. In the extreme, if Θ is allowed to be arbitrarily rich, then $\mathcal{P}_{\text{null}}$ can express any distribution on

¹For example, Kim et al. (2025); Goel et al. (2025) use information about multiple choice answers. In this case, binary correctness is at the answer choice level (i.e., correctly choosing the right answer, or correctly not choosing the wrong answer).

$\{0, 1\}^m$. The next theorem formalizes this observation.² All proofs can be found in Appendix B.

Theorem 1. *For any probability distribution P on $\{0, 1\}^m$, there exists a probability measure H on $[0, 1]^m$ and a latent vector $P_i = (P_{i1}, \dots, P_{im}) \sim H$ such that, conditional on P_i , the coordinates are independent Bernoulli:*

$$Y_{ij} \mid P_i \perp (j = 1, \dots, m), \quad \mathbb{P}(Y_{ij} = 1 \mid P_i) = P_{ij},$$

and the unconditional distribution of Y_i equals P :

$$\mathbb{P}(Y_i = y) = \int \prod_{j=1}^m p_j^{y_j} (1 - p_j)^{1 - y_j} dH(p_1, \dots, p_m).$$

Moreover, there exists a discrete H supported on at most 2^m points with this property.

In other words, there exists a sufficiently expressive null that makes the data look independent conditional on the model parameters Θ . From hereon in this section, we suppress Θ and work directly with abstract families of distributions. All results apply uniformly over any choice of Θ .

3.1. Absorption of Excess Correlation

Theorem 1 hints at the central tension of measuring monoculture: **the more structure we allow the null model to capture, the less apparent correlation remains to be explained.** If the null is too simple, it under-explains the data and makes monoculture appear everywhere; if the null is too rich, it explains away all dependence and makes monoculture impossible to detect. To formalize this idea, we introduce a “null ladder” in Definition 1: a nested sequence of increasingly expressive null models. As we climb the ladder, the null becomes more permissive and the gap between the observed law P and the best-fitting null model must shrink. In Section 3.2, we will instantiate our experiments with two different null ladders with intuitive interpretations.

Definition 1 (Null ladder). Let \mathcal{P} be the set of all laws on $\{0, 1\}^m$. A *null ladder* is a nested sequence $(\mathcal{N}_K)_{K \geq 1}$ with

$$\mathcal{N}_1 \subseteq \mathcal{N}_2 \subseteq \dots \subseteq \mathcal{N}_K \subseteq \mathcal{N}_{K+1} \subseteq \dots \subseteq \mathcal{P}.$$

Definition 2 (Excess at level K). Let $D : \mathcal{P} \times \mathcal{P} \rightarrow [0, \infty)$ be a discrepancy with $D(P, Q) \geq 0$, $D(P, P) = 0$, such as TV distance or f -divergence. For $P \in \mathcal{P}$, define the *minimal excess* at level K and the *best-fitting null*:

$$Q_K^* \in \arg \inf_{Q \in \mathcal{N}_K} D(P, Q), \quad E_{\min}^P(K) := D(P, Q_K^*).$$

When the infimum is not attained, let $(Q_K^*)_{K \geq 1}$ denote any sequence in \mathcal{N}_K satisfying $D(P, Q_K^*) \rightarrow E_{\min}^P(K)$.

²Note that this finite mixture representation is a simple instance of a more general phenomenon: exchangeable or symmetric laws can often be written as mixtures of independent structures, as in de Finetti-type theorems.

The quantity $E_{\min}^P(K)$ measures how much of P remains unexplained at the K th level of the ladder. With this quantity, we can now state our next result, which simply formalizes the intuition that a more expressive model can only explain *more* of the data, never less.

Proposition 2. *For any null ladder (\mathcal{N}_K) and any $P \in \mathcal{P}$,*

$$E_{\min}^P(1) \geq \dots \geq E_{\min}^P(K) \geq E_{\min}^P(K+1) \geq \dots$$

Proposition 2 focuses on the global discrepancy between P and the null, rather than *cross-model correlations* unexplained by the null, which we formalize next. Theorem 3 shows that, provided P can be approximated arbitrarily well along the ladder, these residual covariances vanish as K increases. In other words, a sufficiently rich null model can always reinterpret what appears to be cross-model correlation as arising from latent structure rather than monoculture. We will give an example of such a null ladder next.

Theorem 3. *Fix a parametrized null ladder $(\mathcal{N}_K)_{K \geq 1}$ and let Q_K^* be a best-fitting null law at level K as in Definition 2. Suppose that $D(P, Q_K^*) \xrightarrow{K \rightarrow \infty} 0$, where D is any discrepancy that controls expectations of bounded functions, such as total variation.*

For each K , let $p_{ij}^{(K)} := \Pr_{Q_K^*}(Y_{ij} = 1)$ denote the marginal success probabilities of item i and model j under Q_K^* . Then, for every fixed pair of distinct models $j \neq \ell$,

$$\left| \frac{1}{n} \sum_{i=1}^n \mathbb{E}_P \left[(Y_{ij} - p_{ij}^{(K)}) (Y_{i\ell} - p_{i\ell}^{(K)}) \right] \right| \xrightarrow{K \rightarrow \infty} 0.$$

3.2. Experiments

We now empirically demonstrate Proposition 2 and Theorem 3 by instantiating the null ladder developed in Section 3.1. In particular, we consider two different progressions of complexity in the null model (Experiment 1 and 2). We first introduce the item response theory (IRT) model, which will form our null ladder later.

Item Response Theory (IRT). We use a popular model of capability from psychometrics: *item response theory* (IRT) (Lord, 1980; Embretson & Diehl, 2000). IRT posits that each respondent j possesses a latent ability vector θ_j and that each item i has parameters (a_i, b_i) describing the item’s discrimination and difficulty, respectively. The probability of a correct response is modeled as a strictly increasing function σ (e.g., logit or probit). We note that several recent works apply IRT to evaluating LLMs, see Appendix A for details. Multidimensional IRT (Reckase, 2006) extends this framework by letting θ_j, a_i lie in \mathbb{R}^K . Formally, we have the following null model:

Definition 3 (K -dimensional IRT). Fix $m \geq 1$. For $K \in \mathbb{N}$, let \mathcal{N}_K be the set of laws on $\{0, 1\}^m$ generated by a K -

dimensional latent ability model:

$$p_{ij} = \Pr(Y_{ij} = 1 \mid \theta_j) = \sigma(a_i^\top \theta_j + b_i), \quad Y_{ij} \mid \theta_j \perp \forall j,$$

Crucially, this is a nested family: any distribution representable under a K -dimensional IRT model is also representable under a $(K+1)$ -dimensional model (see Lemma 6). In these experiments, we will set σ to be a probit function.

Throughout, we use IRT as our null model because it provides a simple, intuitive way to incorporate item difficulty while remaining largely dataset-agnostic. Although many alternative null models are possible—e.g., models that account for topic specialization—these typically require additional domain knowledge or assumptions. We therefore use IRT to minimally demonstrate and illustrate our framework.

Datasets. Both experiments will use two datasets following Kim et al. (2025). The first is **HELM** (Liang et al., 2022) (on MMLU data) and the second is the Open LLM Leaderboard on Huggingface³ (from hereon, **HF**). **HELM** has $n = 14,042$ questions over $m = 72$ models, while **HF** has $n = 11,994$ questions over $m = 451$ models. For each, we convert the multiple choice datasets to one of binary correctness responses $Y \in \{0, 1\}^{n \times m}$.

3.2.1. EXPERIMENT 1: INCREASING DIMENSIONS REDUCES EXCESS CORRELATION

Consider a sequence of IRT models with increasing dimensions K . These dimensions can be interpreted as capturing different “types” of questions – for example, mathematical reasoning versus reading comprehension – though we do not impose semantic labels or priors on these dimensions.

Setup. For each $K \in \{1, 2, 4, 8, 16, 32, 36, \dots, 60, 64\}$, we fit a K -dimensional ability model. We estimate the IRT parameters $\{a_i, b_i\}_{i=1}^n$ and $\{\theta_j\}_{j=1}^m$ via gradient-ascent on the joint log-likelihood

$$\ell(a, b, \theta) = \sum_{i=1}^n \sum_{j=1}^m \left[Y_{ij} \log p_{ij} + (1 - Y_{ij}) \log(1 - p_{ij}) \right],$$

with ℓ_2 penalties on a_i , b_i , and θ_j to ensure stability and identifiability. We also apply periodic whitening transformations to θ_j so that the covariance of θ_j remains close to the identity; this removes rotational and scale indeterminacies inherent to IRT models, see (Reckase, 2006) for details. We then recover the estimated probability of correctness (where Φ is the cdf of a standard normal):

$$\hat{p}_{ij}^{(K)} = \Phi\left(\hat{a}_i^{(K)\top} \hat{\theta}_j^{(K)} + \hat{b}_i^{(K)}\right).$$

³<https://huggingface.co/open-llm-leaderboard>

Note that our inference procedure is not intended for out-of-sample prediction, but to describe ability and difficulty within a fixed population. This is standard in IRT models.

Quantities of interest. For each K , we report fit via mean squared error: $\text{MSE}^{(K)} := \frac{1}{nm} \sum_{i=1}^n \sum_{j=1}^m (Y_{ij} - \hat{p}_{ij}^{(K)})^2$. We also define the following quantities:

$$R_{ij}^{(K)} := Y_{ij} - \hat{p}_{ij}^{(K)}, \quad \tilde{R}_{ij}^{(K)} := R_{ij}^{(K)} - \frac{1}{n} \sum_{i=1}^n R_{ij}^{(K)},$$

where R represents the (itemwise) residuals, \tilde{R} is the debiased R to account for calibration error in \hat{p} , see Prop. 7. We then compute the residual covariance matrix \hat{C} :

$$\hat{C}^{(K)} := \frac{1}{n} (\tilde{R}^{(K)})^\top \tilde{R}^{(K)},$$

and obtain the corresponding residual correlation matrix:

$$\hat{\Sigma}^{(K)} := E^{-\frac{1}{2}} \hat{C}^{(K)} E^{-\frac{1}{2}}, \quad E := \text{diag}(\hat{C}^{(K)}) \quad (1)$$

so that $\hat{\Sigma}^{(K)}$ has unit diagonal and is bounded in $[-1, 1]$. $\hat{\Sigma}^{(K)}$ is our measure of excess correlation or monoculture throughout the paper. We will later drop the superscript (K) when the dimensionality K is not relevant. The matrix \hat{C} (and $\hat{\Sigma}$) is a reconstruction of the quantity in Theorem 3. We report the absolute mean in order to summarize the pairwise covariance distribution for each K : $\text{AbsMean}^{(K)} := \frac{1}{m(m-1)} \sum_{j \neq \ell} |\hat{\Sigma}_{j\ell}^{(K)}|$. In Appendix Figure 5, we report additional summary statistics as robustness checks; the general trends still remain.

Results. Figure 1 shows the two quantities of interest (y -axis) across K dimensions of the IRT model (x -axis) on both **HELM** and **HF**. By Proposition 2, enlarging the feasible class from \mathcal{N}_K to \mathcal{N}_{K+1} cannot increase the optimal discrepancy, and we indeed observe a monotone decrease of $\text{MSE}^{(K)}$ as K increases. Similarly, by Theorem 3, we see that the pairwise residual covariances goes to 0 as K increases. This result suggests that unexplained correlation vanishes for sufficiently complex null models. Note that the figures are on a log scale, meaning that increasing dimensions exponentially decreases excess correlation.

3.2.2. EXPERIMENT 2: INCORPORATING ITEM DIFFICULTY REDUCES EXCESS CORRELATION

Setup. We now compare our framework to prior empirical studies of model monoculture that also analyze multiple-choice benchmarks: Goel et al. (2025) and Kim et al. (2025). These works study monoculture relative to baselines that adjust for model-level capability, but their implicit null models **do not incorporate item-level heterogeneity**. Kim et al. (2025) measure agreement rates conditional on both models being incorrect, compared to a null model where all the

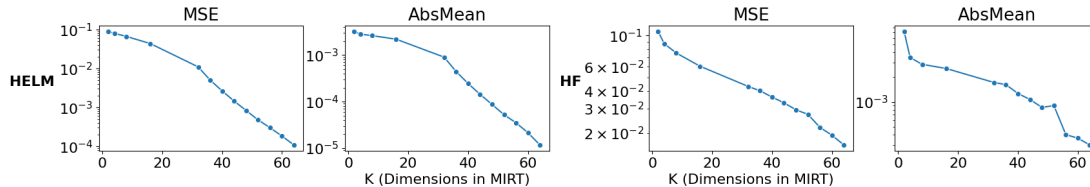


Figure 1. Mean square error (MSE) and absolute mean of the pairwise residual correlations, as a function of K : dimensions in the multidimensional IRT model. Left (right) shows results on the **HELM** (**HF**) dataset. As K increases, residual correlations that are unexplained by the null model tend toward zero, meaning that increasingly expressive null models can arbitrarily absorb model correlations.

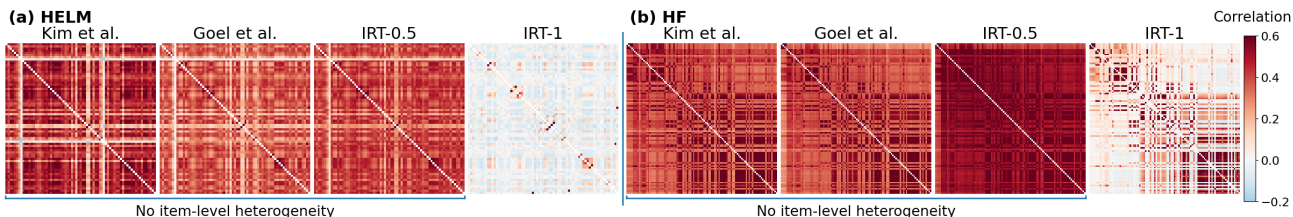


Figure 2. Residual correlation matrices for models in **HELM** (a) and **HF** (b), using different nulls: from left to right, a baseline from Kim et al. (2025), from Goel et al. (2025), from a 1D IRT with no item difficulty, and from a 1D IRT with item difficulties. Each item is a question-answer choice pair. The first three null models **do not** include item heterogeneity. As such, the corresponding excess correlation for the full IRT model is attenuated compared to the others because item difficulties absorb much of the apparent positive correlation.

incorrect choices have an equal probability of being chosen. Meanwhile, Goel et al. (2025) measure how much two models agree on their predicted probabilities beyond what would be expected from their marginal accuracies alone. In our experiments, we do not have access to LLM logits, and so we use the correctness data instead. See Appendix C.2 for details. Both baselines adjust for differences in model capability, but treat all items as exchangeable.

In contrast, we fit two 1-dimensional IRT models, similar to Section 3.2.1.⁴ First, we consider a restricted model in which item difficulty is fixed across all items ($d_i \equiv 0$), so that variation in performance is explained solely by model ability (call this IRT-0.5). This regime serves as our closest analogue to the baselines used by Kim et al. (2025) and Goel et al. (2025), which similarly do not adjust for item-level variation. Second, we fit a full 1-dimensional IRT model with item difficulty parameters, thereby introducing item heterogeneity (IRT-1). The second model is a strictly more expressive null model along the null ladder. By Proposition 2 and Theorem 3, any residual correlations attributable to unmodeled item difficulty should be attenuated when moving from IRT-0.5 to IRT-1.

Results. Figure 2 reports the empirical residual correlation matrices $\hat{\Sigma}$ under constant item difficulty (IRT-0.5) and item

⁴Both Kim et al. (2025) and Goel et al. (2025) use information about multiple choice predictions. So far, we have only considered binary correctness at the question level without the specific answer choices, which indeed provides additional information about cross-model agreement. To provide a similar comparison, we naively fit a 1D IRT model where each observation is a question-answer choice pair. See Appendix C.2 for details. We find similar results compared to fitting on binary correctness data, see Figure 6.

heterogeneity (IRT-1), for both **HELM** and **HF** (restricted to the first 100 models for visualization). Relative to Goel et al. (2025) and Kim et al. (2025), the correlation inferences for IRT-0.5 are slightly higher because it is relatively less expressive: IRT-0.5 only accounts for raw accuracies as a baseline, while both previous works incorporate more specific information about disagreement rates. However, crucially, the correlation inferences under IRT-1 are substantially attenuated compared to the other three, which do not model item heterogeneity – some even flipping from strongly positive to slightly negative. This result highlights the role of increasing expressivity: models may appear correlated simply because they succeed or fail on the same easy or hard questions. When difficulty is explicitly modeled, this apparent agreement is absorbed by the null, revealing a markedly different dependence structure, though the pairwise ordering remains relatively stable. We note that the inferred correlation under IRT-1 for **HELM** and **HF** differ significantly; we explain this difference next.

3.3. Interpreting Monoculture

Thus far, we have established that claims of monoculture are only relative to a null model. Here, we empirically demonstrate that one can interpret the structure of monoculture by fitting a particular null model. We illustrate this idea by fitting a $K = 2$ IRT model to both **HELM** and **HF**, and inspecting the geometry of the resulting latent spaces. This approach allows us to ask what kinds of variation the null absorbs, and what kinds remain unexplained.

Our results are shown in Figure 3. For **HELM**, we find that model abilities largely collapse onto a single dimension that

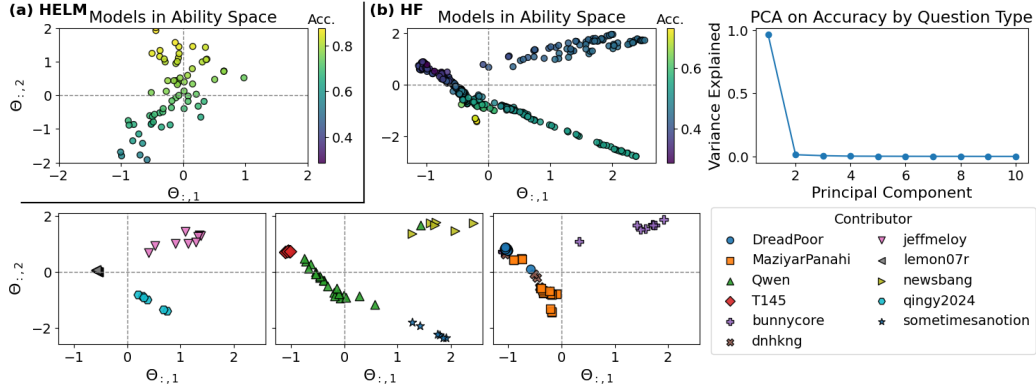


Figure 3. (a) Scatter plot of inferred model ability Θ in a two-dimensional IRT model, colored by accuracy over entire benchmark dataset (**HELM**). (b; top middle) Same as (a), but for **HF** data. (b; top right) Percentage of variance explained by principle component, when applying PCA on model accuracy stratified by question type. (b; bottom) Scatter plot of inferred ability Θ , disaggregated by contributor.

is highly correlated with overall accuracy (subfig. (a)). Once this dimension is accounted for, there is little remaining structured variation across models.

HF (subfig. (b)) presents a more complex picture. Model abilities are more dispersed in the two-dimensional latent space and form distinct clusters that are not strongly correlated with overall accuracy (top middle plot). A natural hypothesis is that these clusters correspond to specialization (e.g., mathematical ability vs reading comprehension). However, a PCA analysis of model accuracies stratified by question type does not support this explanation (top right plot). Instead, the observed clustering appears to be driven by shared provenance among models, such as common contributors or development pipelines (bottom plots). We emphasize, however, that there may be additional factors that explains the heterogeneity beyond what we have explored.

Importantly, these differences should not be read as evidence that one null model is more “appropriate” than another. Rather, they demonstrate how fitting a null model can serve as a diagnostic tool: it makes explicit which priors are consistent with the data and clarifies what residual correlations should be interpreted as. In particular, the differences in correlation structure may reflect differences in model diversity. **HELM** consists primarily of closed-source models, which are likely to share training pipelines, limiting variation in behavior. In contrast, **HF** includes open-source models with more heterogeneous design choices. We build on this observation in the next section.

4. Relativity of Population

In the previous section, we showed that while there is inherent subjectivity in the null model, one can nevertheless fit and defend a reasonable null. In this section, we take that null model as fixed—for example, a one-dimensional IRT model—and interpret *excess correlation* as whatever dependence remains after fitting it.

Our first result (Theorem 4) is that both the fitted null parameters and the resulting excess correlation are **relative to the population of questions and models**. Intuitively, the set of models included in the analysis determines what can be learned about item parameters (e.g., difficulty), while the set of items determines what can be learned about model parameters (e.g., performance). For example, if all questions are trivially easy, models will often correctly agree with each other, and thus it becomes difficult to distinguish between model capability and genuine monoculture.

Our second result highlights the value of evaluating on diverse sets of models and items. Intuitively, greater diversity results in more informative disagreements between models that better reveal the underlying correlation structure. We provide a measure of *stability* and show that when our evaluation context is unstable, we cannot reliably distinguish expected from unexpected agreement.

4.1. Preliminaries

Consider the same setup as described in Section 3.2.1. For notational clarity, we will introduce a more specific parametrization of the null model, $\Theta = (U, V)$, which has the following form:

$$Y_{ij} \mid (U_i, V_j) \perp\!\!\!\perp \forall j, \quad \Pr(Y_{ij} = 1 \mid U_i, V_j) = f(U_i, V_j), \quad (2)$$

where $U_i \in \mathbb{R}^r$ are item factors, $V_j \in \mathbb{R}^r$ are model factors, $f : \mathbb{R}^r \times \mathbb{R}^r \rightarrow (0, 1)$ is a fixed link satisfying mild regularity, and $r \in \mathbb{N}$ is fixed. Note that this includes the IRT models as special cases.

For any choice of item set I and model set J , let $P_{I,J}$ denote the joint distribution of model responses on items I and models J . Let $\mathcal{N}_r(I, J)$ denote the set of distributions that can be explained by an r -dimensional null model (2) using only items I and models J .

Definition 4 (Population-specific target). Given any dis-

crepancy measure $D(P, Q)$ (e.g. TV or an f -divergence), define the *best-fitting null* as

$$Q_{I,J}^* \in \arg \min_{Q \in \mathcal{N}_r(I,J)} D(P_{I,J}, Q). \quad (3)$$

Under Definition 4, any notion of “excess correlation” built from residuals under $Q_{I,J}^*$ is a function of (I, J) . As before, we use Eq. (1) as our notion of excess correlation.

4.2. Inferences depend on the population

It is almost immediate that changing the population changes the null fit, which also changes the residual covariances, as formalized in the following proposition.

Proposition 4 (Population relativity of the null fit). *Fix r and D . The optimizer $Q_{I,J}^*$ in (3) varies as I, J change: there exist item/model sets (I, J) and (I', J') with $I' \subseteq I$ and $J' \subseteq J$ such that the induced marginals do not match,*

$$(Q_{I,J}^*)|_{(I',J')} \neq Q_{I',J'}^*.$$

Here, $(Q_{I,J}^*)|_{(I',J')}$ denotes the marginal predictions for items I' and models J' induced by a null model fit on the larger population (I, J) .

Intuitively, Proposition 4 says that the null model’s inferences depend on the population used to fit it. When the set of items or models changes, the model redistributes explanatory power between these components. In this sense, notions such as difficulty, ability, and excess correlation are not intrinsic properties of isolated models or items, but are defined relative to the population under consideration.

What is the “right” population to choose? For example, if all questions are very similar in difficulty, then we cannot expect to learn much about model behavior. Similarly, if all models behave nearly identically, we cannot distinguish whether they are truly homogeneous or simply being evaluated on trivially easy or hard questions. This intuition suggests that diversity is useful, as we formalize next.

Heterogeneity measure. Let (U^*, V^*) be any fitted null representation achieving $Q_{I,J}^*$ in Defn. 4. Define summary covariance matrices G of the fitted item and model factors,

$$G_U^* := \sum_{i \in I} U_i^* (U_i^*)^\top, \quad G_V^* := \sum_{j \in J} V_j^* (V_j^*)^\top,$$

and use them to measure heterogeneity h :

$$h(I, J) := \min\{\lambda_{\min}(G_U^*), \lambda_{\min}(G_V^*)\}.$$

Here, $\lambda_{\min}(\cdot)$ denotes the smallest eigenvalue, which measures the least amount of variation along any direction in the latent space. Thus, $h(I, J)$ captures the weakest direction of variation across items or models under the fitted null. Larger

$h(I, J)$ means that items and models explore more independent directions in the latent space (i.e., more heterogeneous). As we show in the next result, heterogeneity monotonically improves the conditioning of the null fit.

Theorem 5. *Let $p_{ij}^* = f(U_i^*, V_j^*)$ be the fitted probabilities, where f satisfies standard regularity conditions. For $\varepsilon > 0$, define the ε -equivalence set of latent representations by*

$$\mathcal{E}_\varepsilon := \left\{ (U, V) : \sum_{i \in I} \sum_{j \in J} (f(U_i, V_j) - p_{ij}^*)^2 \leq \varepsilon^2 \right\},$$

modulo invariances of the null model. Then there exists a constant $C > 0$ such that, for all sufficiently small ε ,

$$\sup_{(U,V) \in \mathcal{E}_\varepsilon} \left(\sum_{i \in I} \|U_i - U_i^*\|^2 + \sum_{j \in J} \|V_j - V_j^*\|^2 \right)^{1/2} \leq \frac{C}{\sqrt{h}} \varepsilon.$$

Intuitively, if many items (or models) are similar, the null model has substantial freedom: it can shift latent factors across similar directions without meaningfully changing its predicted probabilities. However, when items and models are diverse, this flexibility disappears: the null parameters become locally well-identified, and the fitted representation is more stable. Thus, having datasets and models with heterogeneity is itself helpful in measuring monoculture.

4.3. Experiments

We now demonstrate Proposition 4 and Theorem 5: that once a null model is fixed, (i) inferred parameters vary depending on the population of interest; and (ii) these inferences are less reliable when the population is homogeneous.

Datasets. We use two datasets: **HELM** as described in Section 3.2, and **ACSIncome** (Ding et al., 2021), which is a prediction task to determine whether an individual earns over \$50,000 based on their demographic attributes. We use this dataset because it allows finer-grained control over model classes and their inductive biases: we train multiple random forests (RF), logistic regression models (LR), and multilayer perceptrons (MLP) on an 80% training split and evaluate them on the held-out 20%. For each model, we convert held-out predictions into a binary correctness variable, which forms the dataset used in our experiment.

Setup. We begin by restricting attention to a subset of models that are expected to be highly correlated due to shared inductive biases. For **ACSIncome**, we first infer $\widehat{\Sigma}$ using only the random forest models; for **HELM**, we start with only OpenAI models, which likely share underlying architectures and training. We then progressively enlarge the population by adding other models and re-estimating $\widehat{\Sigma}$ at each step. In **ACSIncome**, for example, the experiment involves adding logistic regression (LR), then multilayer perceptrons (MLP), then an artificial set of 25 models where

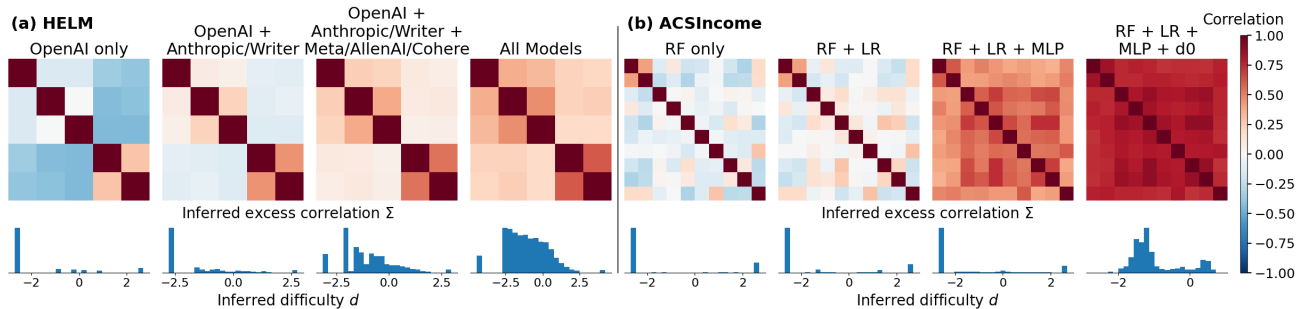


Figure 4. [Top] Inferred excess correlation matrix $\hat{\Sigma}$ from the two-stage procedure, on **HELM** (a) and **ACSIncome** (b) data. For **HELM**, the correlation matrix is shown for OpenAI models only. From left to right, more models are injected into the population for inference, starting from only OpenAI models to all models. For **ACSIncome**, the correlation matrix is shown for random forest models (RF) only, following a similar pattern as **HELM**. [Bottom] Histogram of inferred question difficulties d for all questions in the dataset.

each model has an independent probability of success $p \sim \mathcal{N}(0.7, 0.2)$ (d_0). We include this final step to illustrate the case where “ground truth” item difficulties are all identical, which further increases inferences of excess correlation.

Results. Figure 4 shows that when we restrict the population to a highly correlated subset of models (left subfigures), inferences about correlation reduce to noise. In **ACSIncome** (b), random forests (RF) do not seem correlated despite the inductive biases shared within the model class, since there are no additional disagreements in the dataset to contextualize the agreements within the RF class. Intuitively, the item difficulties we learn correspond to difficulty for *RF models specifically*. Similarly in **HELM** (a), OpenAI models do not seem correlated despite sharing similar base architectures and training data. In these two regimes where models are homogeneous, Thm 5 suggests that many possible (U, V) values can plausibly explain the data, yielding dramatically different inferences about excess agreement. These inferences change as we progressively add more diverse models (as per Prop 4). In particular, we learn a more general notion of difficulty that holds across a broader class of models. This is because more diversity improves the conditioning of our inferences as per Thm 5.

The bottom row of Figure 4, which plots the distribution of inferred item difficulties \hat{d} , further explains this behavior. When the model population is homogeneous, many items are inferred to be very easy or very hard. Without enough disagreement across models, the null model explains agreement by reassigning it to item difficulty rather than to shared model behavior. As more diverse models are introduced, disagreements across models constrain the null fit, spreading \hat{d} distribution more evenly and pushing $\hat{\Sigma}$ up.

5. Discussion

Relative nature of correlation. Claims of model correlation are only valid relative to a well-specified null model. We show that inferences of monoculture are sensitive to

two key choices: (1) the baseline null model; and (2) the population of models and questions. Simple changes in both can dramatically alter what previous works have determined as monoculture (Figs 2 and 4). Researchers should therefore carefully consider and justify these two choices in their evaluations. In particular, our exercise in Section 3.3 can serve as a stepping stone for researchers to better interpret the underlying correlation structure behind their data.

Implications for model multiplicity. Our **ACSIncome** experiments demonstrate how the our framework interacts with the literature on model multiplicity, which studies how distinct models can yield similar predictive performance (Black et al., 2022b). Several studies consider the implications of individual-level arbitrariness (Marx et al., 2020; Gomez et al., 2024; Watson-Daniels et al., 2024; Lee et al., 2024): There are some individuals on whom models agree, and there are others on whom they disagree.

Is this attributable to inherent “difficulty” in classifying those individuals, or is it simply due to monoculture among the class of models under consideration? The answer depends, at least in part, on the population of models chosen. As in Figure 4(b), if the models under consideration are all highly similar, it might appear that certain individuals are simply “obviously low-income,” since every model predicts their income to be low. But as we add heterogeneity to the population of models, these may no longer be obvious classifications. Instead, we see far more heterogeneity in the inferred difficulty of correctly classifying each individual.

Limitations and Future Work. We have shown that conclusions about monoculture are inherently tied to the choice of null model. Our work opens up a natural set of open questions around appropriate selection of a null model, which we hope future work can address. Ultimately, by formalizing the baseline against which agreement is measured, our work provides a path toward distinguishing between the productive consensus of capable systems and the brittle redundancy of algorithmic monoculture.

Impact Statement

Our work contributes to more responsible and interpretable evaluation of AI systems by showing that conclusions about model correlation and monoculture depend critically on modeling assumptions and the given population. By making these dependencies explicit, our framework can help prevent overconfident claims about robustness or diversity, which has broad implications for AI governance and auditing. At the same time, these results underscore the need for careful communication: the relative nature of evaluations should not be used to dismiss genuine risks of correlated failures, but rather to motivate more transparent and large-scale evaluation practices.

References

- Anderson, B. R., Shah, J. H., and Kreminski, M. Homogenization effects of large language models on human creative ideation. In *Proceedings of the 16th conference on creativity & cognition*, pp. 413–425, 2024.
- Baek, J., Bastani, H., and Chen, S. Hiring under congestion and algorithmic monoculture: Value of strategic behavior. *arXiv preprint arXiv:2502.20063*, 2025.
- Black, E., Leino, K., and Fredrikson, M. Selective ensembles for consistent predictions. In *International Conference on Learning Representations*, 2022a.
- Black, E., Raghavan, M., and Barocas, S. Model multiplicity: Opportunities, concerns, and solutions. In *Proceedings of the 2022 ACM conference on fairness, accountability, and transparency*, pp. 850–863, 2022b.
- Black, E., Wang, Z., and Fredrikson, M. Consistent counterfactuals for deep models. In *International Conference on Learning Representations*, 2022c.
- Bommasani, R., Creel, K. A., Kumar, A., Jurafsky, D., and Liang, P. S. Picking on the same person: Does algorithmic monoculture lead to outcome homogenization? *Advances in Neural Information Processing Systems*, 35: 3663–3678, 2022.
- Castleman, J., Nadeem, N., Namjoshi, T., and Liu, L. T. Rethinking math benchmarks for llms using irt. *Proceedings of Machine Learning Research*, 273:66–82, 2025.
- Coston, A., Rambachan, A., and Chouldechova, A. Characterizing fairness over the set of good models under selective labels. In *International Conference on Machine Learning*, pp. 2144–2155. PMLR, 2021.
- Creel, K. and Hellman, D. The algorithmic leviathan: Arbitrariness, fairness, and opportunity in algorithmic decision-making systems. *Canadian Journal of Philosophy*, 52(1):26–43, 2022.
- D’Amour, A., Heller, K., Moldovan, D., Adlam, B., Alipanahi, B., Beutel, A., Chen, C., Deaton, J., Eisenstein, J., Hoffman, M. D., et al. Underspecification presents challenges for credibility in modern machine learning. *Journal of Machine Learning Research*, 23(226):1–61, 2022.
- Ding, F., Hardt, M., Miller, J., and Schmidt, L. Retiring adult: New datasets for fair machine learning. *Advances in neural information processing systems*, 34:6478–6490, 2021.
- Doshi, A. R. and Hauser, O. P. Generative ai enhances individual creativity but reduces the collective diversity of novel content. *Science advances*, 10(28):eadn5290, 2024.
- Embretson, S. E. and Diehl, K. A. *Item response theory*. American Psychological Association, 2000.
- Goel, S., Strüber, J., Auzina, I. A., Chandra, K. K., Kumaraguru, P., Kiela, D., Prabhu, A., Bethge, M., and Geiping, J. Great models think alike and this undermines ai oversight. In *Forty-second International Conference on Machine Learning*, 2025.
- Gomez, J. F., Machado, C., Paes, L. M., and Calmon, F. Algorithmic arbitrariness in content moderation. In *Proceedings of the 2024 ACM Conference on Fairness, Accountability, and Transparency*, pp. 2234–2253, 2024.
- Gorecki, M. and Hardt, M. Monoculture or multiplicity: Which is it? In *The Thirty-ninth Annual Conference on Neural Information Processing Systems*, 2025.
- Jain, S., Suriyakumar, V., Creel, K., and Wilson, A. Algorithmic pluralism: A structural approach to equal opportunity. In *Proceedings of the 2024 ACM Conference on Fairness, Accountability, and Transparency*, pp. 197–206, 2024.
- Jo, N., Wilson, A., Creel, K. A., and Raghavan, M. Homogeneous algorithms can reduce competition in personalized pricing. In *Advances in Neural Information Processing Systems*, 2025.
- Kim, E. M., Garg, A., Peng, K., and Garg, N. Correlated errors in large language models. In *Forty-second International Conference on Machine Learning*, 2025.
- Kleinberg, J. and Raghavan, M. Algorithmic monoculture and social welfare. *Proceedings of the National Academy of Sciences*, 118(22):e2018340118, 2021.
- Lee, J., Harvey, E., Zhou, J., Garg, N., Joachims, T., and Kizilcec, R. F. Ending affirmative action harms diversity without improving academic merit. In *Proceedings of the 4th ACM Conference on Equity and Access in Algorithms, Mechanisms, and Optimization*,

- EAAMO '24, New York, NY, USA, 2024. Association for Computing Machinery. ISBN 9798400712227. doi: 10.1145/3689904.3694706. URL <https://doi.org/10.1145/3689904.3694706>.
- Liang, P., Bommasani, R., Lee, T., Tsipras, D., Soylu, D., Yasunaga, M., Zhang, Y., Narayanan, D., Wu, Y., Kumar, A., et al. Holistic evaluation of language models. *arXiv preprint arXiv:2211.09110*, 2022.
- Lord, F. M. *Applications of Item Response Theory to Practical Testing Problems*. ERIC, 1980.
- Maia Polo, F., Weber, L., Choshen, L., Sun, Y., Xu, G., and Yurochkin, M. tinyBenchmarks: evaluating LLMs with fewer examples. In Salakhutdinov, R., Kolter, Z., Heller, K., Weller, A., Oliver, N., Scarlett, J., and Berkenkamp, F. (eds.), *Proceedings of the 41st International Conference on Machine Learning*, volume 235 of *Proceedings of Machine Learning Research*, pp. 34303–34326. PMLR, 21–27 Jul 2024. URL <https://proceedings.mlr.press/v235/maia-polo24a.html>.
- Martínez-Plumed, F., Prudêncio, R. B., Martínez-Usó, A., and Hernández-Orallo, J. Item response theory in ai: Analysing machine learning classifiers at the instance level. *Artificial intelligence*, 271:18–42, 2019.
- Marx, C., Calmon, F., and Ustun, B. Predictive multiplicity in classification. In *International conference on machine learning*, pp. 6765–6774. PMLR, 2020.
- Padmakumar, V. and He, H. Does writing with language models reduce content diversity? In *The Twelfth International Conference on Learning Representations*, 2024. URL <https://openreview.net/forum?id=Feiz5HtCD0>.
- Pawelczyk, M., Broelemann, K., and Kasneci, G. On counterfactual explanations under predictive multiplicity. In *Conference on Uncertainty in Artificial Intelligence*, pp. 809–818. PMLR, 2020.
- Peng, K. and Garg, N. Monoculture in matching markets. In *The Thirty-eighth Annual Conference on Neural Information Processing Systems*, 2024a. URL <https://openreview.net/forum?id=P5yezHuMSS>.
- Peng, K. and Garg, N. Wisdom and foolishness of noisy matching markets. In *Proceedings of the 25th ACM Conference on Economics and Computation*, pp. 675–675, 2024b.
- Raghavan, M. Competition and diversity in generative ai. *arXiv preprint arXiv:2412.08610*, 2024.
- Reckase, M. D. Multidimensional item response theory. *Handbook of statistics*, 26:607–642, 2006.
- Rodolfa, K. T., Lamba, H., and Ghani, R. Empirical observation of negligible fairness–accuracy trade-offs in machine learning for public policy. *Nature Machine Intelligence*, 3(10):896–904, 2021.
- Rodriguez, P., Barrow, J., Hoyle, A. M., Lalor, J. P., Jia, R., and Boyd-Graber, J. Evaluation examples are not equally informative: How should that change nlp leaderboards? In *Proceedings of the 59th Annual Meeting of the Association for Computational Linguistics and the 11th International Joint Conference on Natural Language Processing (Volume 1: Long Papers)*, pp. 4486–4503, 2021.
- Schilling-Wilhelmi, M., Alampara, N., and Jablonka, K. M. Lifting the benchmark iceberg with item-response theory. In *AI for Accelerated Materials Design-ICLR 2025*, 2025.
- Semenova, L., Rudin, C., and Parr, R. On the existence of simpler machine learning models. In *Proceedings of the 2022 ACM Conference on Fairness, Accountability, and Transparency*, pp. 1827–1858, 2022.
- Toups, C., Bommasani, R., Creel, K., Bana, S., Jurafsky, D., and Liang, P. S. Ecosystem-level analysis of deployed machine learning reveals homogeneous outcomes. *Advances in Neural Information Processing Systems*, 36: 51178–51201, 2023.
- Ugander, J. and Epstein, Z. The art of randomness: Sampling and chance in the age of algorithmic reproduction. *Harvard Data Science Review*, 6(4), 2024.
- Watson-Daniels, J., Calmon, F. d. P., D’Amour, A., Long, C., Parkes, D. C., and Ustun, B. Predictive churn with the set of good models. *arXiv preprint arXiv:2402.07745*, 2024.
- Wenger, E. and Kenett, Y. We’re different, we’re the same: Creative homogeneity across llms. *arXiv preprint arXiv:2501.19361*, 2025.
- Wu, F., Black, E., and Chandrasekaran, V. Generative monoculture in large language models. In *The Thirteenth International Conference on Learning Representations*, 2025.
- Zhou, H., Huang, H., Zhao, Z., Han, L., Wang, H., Chen, K., Yang, M., Bao, W., Dong, J., Xu, B., et al. Lost in benchmarks? rethinking large language model benchmarking with item response theory. *arXiv preprint arXiv:2505.15055*, 2025.

A. Other Related Work

Model Evaluations using IRT. While our results apply broadly to any choice of null models, in this work we often use IRT models as a null because they incorporate item-level heterogeneity. Many recent works have used IRT in their evaluations (Martínez-Plumed et al., 2019; Rodríguez et al., 2021; Maia Polo et al., 2024; Schilling-Wilhelmi et al., 2025; Zhou et al., 2025; Castleman et al., 2025), acknowledging that questions vary in characteristics and some may be more informative than others. However, all of these works use IRT in the context of evaluating model capabilities rather than, as we do, inter-model correlations.

Model Multiplicity. Model multiplicity suggests that highly expressive models admit many different solutions that are consistent with the same training data, often reflecting different inductive biases or arbitrary choices among equivalent hypotheses (Black et al., 2022b; Marx et al., 2020). There have been many works that seek to characterize or mitigate multiplicity across a variety of contexts (Pawelczyk et al., 2020; Rodolfa et al., 2021; Coston et al., 2021; D’Amour et al., 2022; Semenova et al., 2022; Black et al., 2022c;a). In these works, multiplicity is typically framed as a property of the *model class*: more flexible hypotheses allow for a greater number of solutions. However, our results suggest another perspective in which multiplicity is also shaped by *the population of models used for evaluation*. We discuss this further in Section 5.

B. Additional Theorems and Proofs

B.1. Additional Results

Lemma 6 (Nestedness of ability nulls). *For all K , we have $\mathcal{N}_K \subseteq \mathcal{N}_{K+1}$.*

Proof. Embed the K -dimensional latent θ_i into \mathbb{R}^{K+1} by $\theta'_i = (\theta_i, 0)$ and extend $a'_j = (a_j, 0)$. Then $\sigma(a'_i{}^\top \theta'_j + b_i) = \sigma(a_i{}^\top \theta_j + b_i)$, so every law representable at dimension K is also representable at $K+1$. \square

Proposition 7 (Debiasing residuals removes calibration error). *Let $Y_{ij} \in \{0, 1\}$ denote the observed response for item $i \in \{1, \dots, n\}$ and model/respondent $j \in \{1, \dots, m\}$. Assume the item rows $Y_i = (Y_{i1}, \dots, Y_{im})$ are i.i.d. from some law P . For each (i, j) , let $p_{ij}^* := \Pr(Y_{ij} = 1)$ denote the true success probability and let $\hat{p}_{ij} \in (0, 1)$ be any (possibly misspecified) model-based estimate of p_{ij}^* .*

Define the raw residual

$$e_{ij} := Y_{ij} - \hat{p}_{ij},$$

and, for a fixed model j , define the sample mean residual across items

$$\bar{e}_{\cdot j} := \frac{1}{n} \sum_{i=1}^n e_{ij} = \frac{1}{n} \sum_{i=1}^n (Y_{ij} - \hat{p}_{ij}).$$

Then the population mean of the raw residual equals the population calibration error:

$$\mathbb{E}[e_{ij}] = \mathbb{E}[Y_{ij} - \hat{p}_{ij}] = \mathbb{E}[p_{ij}^* - \hat{p}_{ij}].$$

Moreover, by the law of large numbers,

$$\bar{e}_{\cdot j} \xrightarrow{P} \mathbb{E}[p_{ij}^* - \hat{p}_{ij}] \quad \text{as } n \rightarrow \infty,$$

so $\bar{e}_{\cdot j}$ is a consistent estimator of the (model- j) average calibration error across items.

Consequently, the debaised residual

$$\tilde{e}_{ij} := e_{ij} - \bar{e}_{\cdot j} = (Y_{ij} - \hat{p}_{ij}) - \frac{1}{n} \sum_{i'=1}^n (Y_{i'j} - \hat{p}_{i'j})$$

satisfies

$$\mathbb{E}[\tilde{e}_{ij}] \approx 0$$

for large n , and, in the limit $n \rightarrow \infty$,

$$\tilde{e}_{ij} \approx Y_{ij} - p_{ij}^*,$$

i.e. it removes the model-specific calibration bias and leaves only the zero-mean Bernoulli fluctuation.

In particular, sample covariances (or correlations) computed from the debiased residuals \tilde{e}_{ij} estimate the residual dependence across models, rather than spurious correlations induced by shared calibration error.

B.2. Proofs

Proof of Theorem 1.

Proof. Define a discrete probability measure H^* on the vertices $\{0, 1\}^m \subset [0, 1]^m$ by placing mass $P(y)$ at the point $p = y$: $H^*(\{y\}) = P(y)$ for each $y \in \{0, 1\}^m$. Given $P_i \sim H^*$, define the conditional law of Y_i by independent Bernoulli coordinates with success probabilities P_{ij} :

$$\mathbb{P}(Y_{ij} = 1 \mid P_i = p) = p_j, \quad j = 1, \dots, m.$$

If $P_i = y \in \{0, 1\}^m$, then each Y_{ij} is almost surely equal to y_j , so

$$\mathbb{P}(Y_i = y \mid P_i = y) = \prod_{j=1}^m y_j^{y_j} (1 - y_j)^{1 - y_j} = 1.$$

Integrating over H^* gives, for any $y \in \{0, 1\}^m$,

$$\mathbb{P}(Y_i = y) = \int \mathbb{P}(Y_i = y \mid P_i = p) dH^*(p) = \sum_{y' \in \{0, 1\}^m} \mathbb{I}\{y' = y\} P(y') = P(y).$$

Thus P admits the desired mixture representation with $H = H^*$. By construction, H^* is supported on at most 2^m points. \square

Proof of Proposition 2.

Proof. Fix K and distinct $j \neq \ell$. Define the function $g_K : \{0, 1\}^{n \times m} \rightarrow \mathbb{R}$ by

$$g_K(y) := \frac{1}{n} \sum_{i=1}^n (y_{ij} - p_{ij}^{(K)})(y_{i\ell} - p_{i\ell}^{(K)}).$$

Since each $y_{ij} \in \{0, 1\}$ and $p_{ij}^{(K)} \in [0, 1]$, we have $|y_{ij} - p_{ij}^{(K)}| \leq 1$, hence

$$|g_K(y)| \leq \frac{1}{n} \sum_{i=1}^n 1 = 1 \quad \text{for all } y,$$

so $\|g_K\|_\infty \leq 1$.

By definition of the null model in Section 2, for each item i ,

$$\mathbb{E}_{Q_K^*} \left[(Y_{ij} - p_{ij}^{(K)})(Y_{i\ell} - p_{i\ell}^{(K)}) \right] = \mathbb{E}_{Q_K^*} [Y_{ij} - p_{ij}^{(K)}] \mathbb{E}_{Q_K^*} [Y_{i\ell} - p_{i\ell}^{(K)}] = 0,$$

because $\mathbb{E}_{Q_K^*} [Y_{ij} - p_{ij}^{(K)}] = \Pr_{Q_K^*}(Y_{ij} = 1) - p_{ij}^{(K)} = 0$. Averaging over i gives $\mathbb{E}_{Q_K^*} [g_K(Y)] = 0$.

Therefore,

$$|\mathbb{E}_P [g_K(Y)]| = |\mathbb{E}_P [g_K(Y)] - \mathbb{E}_{Q_K^*} [g_K(Y)]|.$$

Now use the standard total variation inequality: for any two probability laws μ, ν on a finite measurable space and any f with $\|f\|_\infty \leq 1$,

$$|\mathbb{E}_\mu [f] - \mathbb{E}_\nu [f]| \leq 2 \text{TV}(\mu, \nu).$$

Applying this with $\mu = P$, $\nu = Q_K^*$, and $f = g_K$ yields

$$|\mathbb{E}_P[g_K(Y)]| \leq 2 \text{TV}(P, Q_K^*).$$

Finally, note that $\mathbb{E}_P[g_K(Y)]$ is exactly the left-hand side quantity:

$$\mathbb{E}_P[g_K(Y)] = \frac{1}{n} \sum_{i=1}^n \mathbb{E}_P[(Y_{ij} - p_{ij}^{(K)})(Y_{i\ell} - p_{i\ell}^{(K)})].$$

The claimed bound follows, and since $\text{TV}(P, Q_K^*) \rightarrow 0$ by assumption, the left-hand side converges to 0. \square

Remark 1. Theorem 3 is stated in terms of the model-implied probabilities $p_{ij}^{(K)}$. In practice we use fitted probabilities $\hat{p}_{ij}^{(K)}$ obtained from the K -dimensional IRT fit. Under standard consistency of the estimator within \mathcal{N}_K , the sample residual cross-item correlations computed from $\hat{p}_{ij}^{(K)}$ converge in probability to the population quantities in the corollary, and thus shrink toward 0 as K grows.

Proof of Proposition 4.

Proof. The key observation is that the best-fitting null model is defined *relative to the population* through the optimization problem (3). Changing the item or model set changes both the feasible set $\mathcal{N}_r(I, J)$ and the objective being minimized.

Fix (I, J) and suppose $Q_{I,J}^*$ is a minimizer of $D(P_{I,J}, Q)$ over $\mathcal{N}_r(I, J)$. By construction, the parameters (U, V) underlying $Q_{I,J}^*$ must jointly explain *all* item–model interactions in (I, J) using a shared r -dimensional representation. In particular, the fitted parameters for items in I' and models in J' are influenced by the presence of additional items $I \setminus I'$ and models $J \setminus J'$ through this shared low-dimensional constraint.

Now consider fitting the null model directly on the restricted population (I', J') . The optimizer $Q_{I',J'}^*$ is free to choose parameters that best explain $P_{I',J'}$ alone, without needing to simultaneously accommodate the behavior of items or models outside this subset. Unless the restriction of $Q_{I,J}^*$ to (I', J') already happens to be optimal for this smaller problem—which would require a special compatibility condition—there is no reason for the induced marginal $(Q_{I,J}^*)|_{(I',J')}$ to coincide with $Q_{I',J'}^*$.

Therefore, there exist populations (I, J) and strict subsets (I', J') for which

$$(Q_{I,J}^*)|_{(I',J')} \neq Q_{I',J'}^*,$$

establishing that the null fit, and hence any residual-based notion of excess correlation, depends on the chosen population. \square

Proof of Theorem 5.

Proof. Write perturbations

$$\Delta U_i := U_i - U_i^*, \quad \Delta V_j := V_j - V_j^*, \quad \Delta p_{ij} := f(U_i, V_j) - p_{ij}^*.$$

Let $\|\Delta U\|_F^2 := \sum_{i \in I} \|\Delta U_i\|^2$ and $\|\Delta V\|_F^2 := \sum_{j \in J} \|\Delta V_j\|^2$, and set

$$\|(\Delta U, \Delta V)\|^2 := \|\Delta U\|_F^2 + \|\Delta V\|_F^2.$$

Regularity and the heterogeneity index. Recall (from the definition of h in the text) that

$$G_U^* := \sum_{i \in I} U_i^*(U_i^*)^\top, \quad G_V^* := \sum_{j \in J} V_j^*(V_j^*)^\top, \quad h := \min\{\lambda_{\min}(G_U^*), \lambda_{\min}(G_V^*)\}.$$

Under the “standard regularity conditions” assumed in the statement, we may fix a neighborhood \mathcal{N} of (U^*, V^*) on which the following hold:

(R1) f is continuously differentiable and its partial derivatives are uniformly bounded and bounded away from 0 along the fitted margins, i.e. there exists $m > 0$ such that

$$\|\nabla_u f(U_i, V_j)\| \geq m, \quad \|\nabla_v f(U_i, V_j)\| \geq m \quad \forall (U, V) \in \mathcal{N}, \forall i, j.$$

(R2) The first-order Taylor remainder is uniformly quadratic: there exists $L < \infty$ such that for all $(U, V) \in \mathcal{N}$ and all i, j ,

$$|f(U_i, V_j) - f(U_i^*, V_j^*) - \langle \nabla_u f(U_i^*, V_j^*), \Delta U_i \rangle - \langle \nabla_v f(U_i^*, V_j^*), \Delta V_j \rangle| \leq L(\|\Delta U_i\| + \|\Delta V_j\|)^2.$$

(R3) The derivatives align with the fitted latent directions in the sense that there exist matrices $A_{ij}, B_{ij} \in \mathbb{R}^{r \times r}$, uniformly well-conditioned on \mathcal{N} , such that

$$\nabla_u f(U_i^*, V_j^*) = A_{ij} V_j^*, \quad \nabla_v f(U_i^*, V_j^*) = B_{ij} U_i^*,$$

and $\lambda_{\min}(A_{ij}^\top A_{ij}) \geq m^2$, $\lambda_{\min}(B_{ij}^\top B_{ij}) \geq m^2$ for all i, j . (This condition holds for standard IRT/MIRT links, where $f(u, v) = g(u^\top v)$ and $A_{ij} = B_{ij} = g'((U_i^*)^\top V_j^*) I$.)

All constants below depend only on (m, L) and the bounds implicit in (R1)–(R3), and not on ε .

Step 1: Reduce $\|\Delta p\|_2$ to the linearization. Define the linearized change

$$\Delta p_{ij}^{\text{lin}} := \langle \nabla_u f(U_i^*, V_j^*), \Delta U_i \rangle + \langle \nabla_v f(U_i^*, V_j^*), \Delta V_j \rangle.$$

By (R2),

$$|\Delta p_{ij} - \Delta p_{ij}^{\text{lin}}| \leq L(\|\Delta U_i\| + \|\Delta V_j\|)^2.$$

Summing squares and using $(a - b)^2 \geq \frac{1}{2}a^2 - b^2$ yields, for (U, V) sufficiently close to (U^*, V^*) (equivalently, for $\|(\Delta U, \Delta V)\|$ small enough),

$$\sum_{i,j} \Delta p_{ij}^2 \geq \frac{1}{2} \sum_{i,j} (\Delta p_{ij}^{\text{lin}})^2. \quad (1)$$

(Indeed, the quadratic remainder contributes $O(\|(\Delta U, \Delta V)\|^4)$, which is dominated by the linear term in a small neighborhood.)

Step 2: Lower bound the linear term using h . Using (R3), write

$$\Delta p_{ij}^{\text{lin}} = \langle A_{ij} V_j^*, \Delta U_i \rangle + \langle B_{ij} U_i^*, \Delta V_j \rangle.$$

Apply $(a + b)^2 \geq \frac{1}{4}a^2 + \frac{1}{4}b^2$ to obtain

$$(\Delta p_{ij}^{\text{lin}})^2 \geq \frac{1}{4} \langle A_{ij} V_j^*, \Delta U_i \rangle^2 + \frac{1}{4} \langle B_{ij} U_i^*, \Delta V_j \rangle^2. \quad (2)$$

Summing (2) over (i, j) and using the uniform conditioning in (R3),

$$\sum_{i,j} (\Delta p_{ij}^{\text{lin}})^2 \geq \frac{1}{4} m^2 \sum_{i,j} \langle V_j^*, \Delta U_i \rangle^2 + \frac{1}{4} m^2 \sum_{i,j} \langle U_i^*, \Delta V_j \rangle^2.$$

Now,

$$\sum_{j \in J} \langle V_j^*, \Delta U_i \rangle^2 = (\Delta U_i)^\top \left(\sum_{j \in J} V_j^* (V_j^*)^\top \right) \Delta U_i = (\Delta U_i)^\top G_V^* \Delta U_i \geq \lambda_{\min}(G_V^*) \|\Delta U_i\|^2,$$

and summing over i gives

$$\sum_{i,j} \langle V_j^*, \Delta U_i \rangle^2 \geq \lambda_{\min}(G_V^*) \sum_i \|\Delta U_i\|^2.$$

Similarly,

$$\sum_{i,j} \langle U_i^*, \Delta V_j \rangle^2 \geq \lambda_{\min}(G_U^*) \sum_j \|\Delta V_j\|^2.$$

Combining these bounds and recalling the definition of h yields

$$\sum_{i,j} (\Delta p_{ij}^{\text{lin}})^2 \geq \frac{1}{4} m^2 h \left(\|\Delta U\|_F^2 + \|\Delta V\|_F^2 \right) = \frac{1}{4} m^2 h \|(\Delta U, \Delta V)\|^2. \quad (3)$$

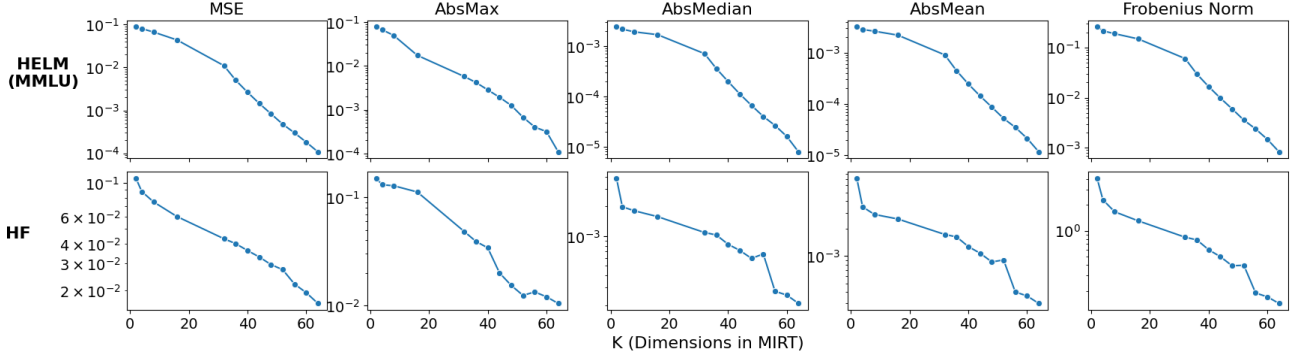


Figure 5. Mean square error (MSE) and summary statistics of the distribution of pairwise residual correlations, as a function of K : the dimensions in the multidimensional IRT model. Top (bottom) row shows results on the **HELM (HF)** dataset. As K increases, the residual correlations that are unexplained by the independent null model tend toward zero, meaning that a sufficiently expressive null model can arbitrarily absorb model correlations.

Step 3: Conclude the shrinkage bound for \mathcal{E}_ε . Combining (1) and (3) gives, for (U, V) sufficiently close to (U^*, V^*) ,

$$\sum_{i,j} \Delta p_{ij}^2 \geq \frac{1}{2} \sum_{i,j} (\Delta p_{ij}^{\text{lin}})^2 \geq \frac{m^2 h}{8} \|(\Delta U, \Delta V)\|^2.$$

Now take any $(U, V) \in \mathcal{E}_\varepsilon \cap \mathcal{N}$. By definition, $\sum_{i,j} \Delta p_{ij}^2 \leq \varepsilon^2$, hence

$$\|(\Delta U, \Delta V)\|^2 \leq \frac{8}{m^2 h} \varepsilon^2, \quad \text{so} \quad \|(\Delta U, \Delta V)\| \leq \frac{\sqrt{8}}{m\sqrt{h}} \varepsilon.$$

Therefore the stated bound holds with $C = \sqrt{8}/m$ (and after quotienting by the invariances of the null model, as in the statement). This proves that the diameter of \mathcal{E}_ε in the parameter norm is $O(\varepsilon/\sqrt{h})$, and hence increasing h monotonically shrinks \mathcal{E}_ε . \square

C. Experiment Details from Section 3

C.1. Experiment 1 (Extensions)

In order to summarize the pairwise covariance distribution, we compute the following summary statistics from C for each K :

$$\begin{aligned} \text{(i) AbsMax}^{(K)} &:= \max_{j \neq \ell} |\widehat{\Sigma}_{j\ell}^{(K)}|, & \text{(ii) AbsMean}^{(K)} &:= \frac{1}{m(m-1)} \sum_{j \neq \ell} |\widehat{\Sigma}_{j\ell}^{(K)}|, \\ \text{(iii) Median}^{(K)} &:= \text{median}_{j \neq \ell} |\widehat{\Sigma}_{j\ell}^{(K)}|, & \text{(iv) } \|\widehat{\Sigma}^{(K)}\|_{\text{off}, F} &:= \sqrt{\sum_{j \neq \ell} (\widehat{\Sigma}_{j\ell}^{(K)})^2}. \end{aligned}$$

We summarize our results in Figure 5. As in Theorem 3, the pairwise residual correlations tend to zero as K becomes arbitrarily large.

C.2. Experiment 2 (Details)

Baselines from prior work. Both Kim et al. (2025) and Goel et al. (2025) operate on multiple-choice data. Let $A_{ij} \in \{1, \dots, K_i\}$ denote the option selected by model j on item i , with correct option a_i^* .

Kim et al. focus on agreement conditional on both models being incorrect:

$$q_{j\ell} := \Pr(A_{ij} = A_{i\ell} \mid A_{ij} \neq a_i^*, A_{i\ell} \neq a_i^*),$$

and compare this quantity to the chance baseline

$$q_{j\ell}^{\text{ch}} := \mathbb{E} \left[\frac{1}{K_i - 1} \right],$$

which corresponds to uniform random selection among the incorrect options. Excess correlation is defined as the difference between these two quantities:

$$\text{Excess} := q_{j\ell} - q_{j\ell}^{\text{ch}}$$

$$\kappa_{j\ell}^{\text{err}} := \frac{q_{j\ell} - q_{j\ell}^{\text{ch}}}{1 - q_{j\ell}^{\text{ch}}}$$

Goel *et al.* define a probabilistic agreement measure based on the inner product of predictive distributions. In the discrete (argmax-only) setting, their observed agreement reduces to

$$c_{\text{obs}} = \frac{1}{n} \sum_{i=1}^n \mathbf{1}\{A_{ij} = A_{i\ell}\},$$

while their chance agreement baseline is

$$c_{\text{exp}} = p_j p_\ell + (1 - p_j)(1 - p_\ell) \mathbb{E} \left[\frac{1}{K_i - 1} \right],$$

where p_j denotes model j 's overall accuracy. Their CAPA statistic is a normalized excess-over-chance measure,

$$\text{CAPA}_{j\ell} = \frac{c_{\text{obs}} - c_{\text{exp}}}{1 - c_{\text{exp}}}.$$

Both baselines adjust for differences in model capability, but treat all items as exchangeable.

Our null: 1-dimensional IRT on multiple-choice correctness. We now evaluate excess correlation using a strictly more expressive null model. Specifically, we fit a *1-dimensional IRT model* ($K = 1$) to the same multiple-choice data, where

$$Y_{ij} := \mathbf{1}\{A_{ij} = a_i^*\}$$

indicates whether model j selected the correct option on item i . The null model is

$$\Pr(Y_{ij} = 1) = \Phi(a_i \theta_j + b_i),$$

with item-specific difficulty and discrimination parameters (a_i, b_i) and model ability θ_j .

This model strictly subsumes the baselines above: if all items share identical parameters, the IRT model reduces to a capability-only model, whereas allowing (a_i, b_i) to vary introduces item heterogeneity. Thus, in the language of Section 3.1, this represents a higher rung in the null ladder.

Residual dependence. After fitting the model, we compute residuals

$$R_{ij} = Y_{ij} - \hat{p}_{ij},$$

de-bias them as in Experiment 1, and estimate the residual covariance matrix

$$\hat{C} = \frac{1}{n} \tilde{R}^\top \tilde{R}.$$

This quantity captures excess model-to-model dependence not explained by either model ability or item difficulty.

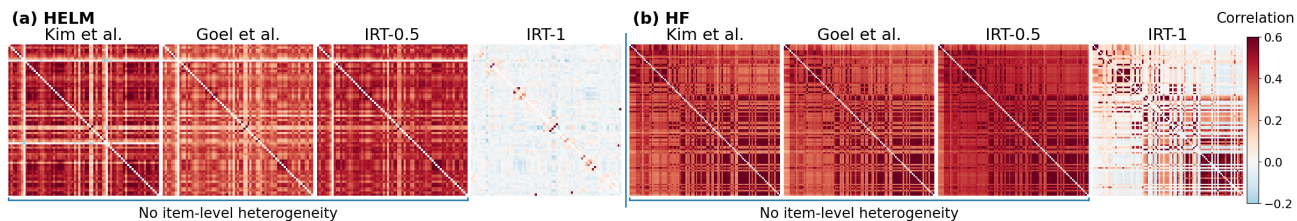


Figure 6. Residual correlation matrices for models in **HELM** (a) and **HF** (b), using different nulls: from left to right, a baseline from Kim et al. (2025), from Goel et al. (2025), from a 1D IRT with no item difficulty, and from a 1D IRT with item difficulties. Each item is a question. The first three null models **do not** include item heterogeneity. As such, the corresponding excess correlation for the full IRT model is attenuated compared to the others because item difficulties absorb much of the apparent positive correlation.

C.2.1. ADDITIONAL RESULTS

In Figure 2, we used a null model where each item is a (question, answer-choice) pair in order to provide a fair comparison to previous methods. In Figure 6, we use a null model where each item is at the question level. The results do not change significantly, indicating that our findings remain robust to the choice of null model.

D. Extensions

D.1. Generalizing to other output spaces

The framework accommodates a wide range of choices for \mathcal{Y} , including:

- (1) **Binary correctness:** $\mathcal{Y} = \{0, 1\}$, where $Y_{ij} = 1$ denotes a correct answer.
- (2) **Probabilistic correctness:** $\mathcal{Y} = [0, 1]$, where Y_{ij} is a calibrated probability of correctness.
- (3) **Logits or score vectors:** $\mathcal{Y} = \mathbb{R}^V$, such as the model’s pre-softmax logits over a vocabulary of size V .
- (4) **Natural language:** $\mathcal{Y} = \mathcal{T}^*$, the space of token sequences.

Generalizing to probabilistic correctness is immediate: one simply replaces each Bernoulli variable with a real value in $[0, 1]$ and defines independence conditional on latent parameters in the same manner. Richer output spaces (logits and natural language) require more care. For logits, one natural approach is to view each Y_{ij} as a vector of real-valued features and study conditional independence of these vectors given latent parameters. For natural language, a possible strategy is to embed outputs via a mapping $f : \mathcal{T}^* \rightarrow \mathbb{R}^d$ (e.g. semantic or style embeddings) and treat the embedded representations $X_{ij} = f(Y_{ij})$ as the objects of analysis. In this case, an “independent” null model would posit that, conditional on latent structure, these embeddings are independent across models. However, the appropriate parameterization of such latent structure (e.g. global factors capturing topic, stylistic preferences, or discourse-level strategies) is not yet clear and presents an interesting direction for future work.

D.2. Inferring Σ

In this work, we define and calculate monoculture Σ as the pairwise correlations of the residuals between the outcomes Y and the null model fitted probabilities \hat{p} . This gives us a metric that is agnostic to the particular inference algorithm used to infer Σ . However, one may want to directly infer Σ from the data, and in this section we provide one principles way of doing so.

Kernel parameterization and estimation of Σ . We first introduce a latent Gaussian variable Z_{ij} , where $Y_{ij} = \mathbb{I}[Z_{ij} \geq 0]$. We can therefore equivalently re-write the generative model as:

$$Z_{ij} = \theta_j - b_i + \varepsilon_{ij}, \quad \varepsilon_{.j} \sim \mathcal{N}(0, \Sigma), \tag{4}$$

where for each item i the vector $\varepsilon_i \in \mathbb{R}^M$ (across M models) has covariance matrix $\Sigma \in \mathbb{R}^{M \times M}$, shared across items. The null model corresponds to $\Sigma = I_M$, i.e., conditionally independent models given (θ, b) . Any deviation $\Sigma \neq I_M$ is

interpreted as *excess correlation* between models beyond what is induced by sharing the same item difficulties and model abilities.

In the alternative model (4), assume the excess-correlation matrix $\Sigma \in \mathbb{R}^{M \times M}$ is parameterized via low-dimensional embeddings for each model. Let $v_j \in \mathbb{R}^K$ denote the embedding for model j , and let $V \in \mathbb{R}^{M \times K}$ collect these row-wise. We define pairwise correlations by

$$\rho_{jk} = v_j^\top v_k, \quad j \neq k,$$

and enforce unit variance by setting

$$\Sigma = VV^\top + \text{diag}(1 - \|v_1\|_2^2, \dots, 1 - \|v_M\|_2^2). \quad (5)$$

If we maintain $\|v_j\|_2 \leq 1$ for all j , then Σ is positive semidefinite and has unit diagonal:

$$\Sigma_{jj} = \|v_j\|_2^2 + (1 - \|v_j\|_2^2) = 1.$$

In the implementation, we explicitly use $\rho_{jk} = v_j^\top v_k$ for $j \neq k$ in the bivariate probit calculations and fix $\Sigma_{jj} = 1$ via (5).

Model-implied and empirical covariances. Let $Y \in \{0, 1\}^{N \times M}$ be the correctness matrix (items \times models), and let $(\hat{\theta}, \hat{b})$ be the 1D IRT estimates from Stage 1. Define

$$\hat{\mu}_{ij} = \hat{\theta}_j - \hat{b}_i, \quad \hat{p}_{ij} = \Phi(\hat{\mu}_{ij}), \quad \hat{m}_j = \frac{1}{N} \sum_{i=1}^N \hat{p}_{ij}, \quad \bar{Y}_j = \frac{1}{N} \sum_{i=1}^N Y_{ij}.$$

For a given pair (j, k) and correlation ρ_{jk} , the latent pair (Z_{ij}, Z_{ik}) for item i is modeled as

$$\begin{pmatrix} Z_{ij} \\ Z_{ik} \end{pmatrix} \sim \mathcal{N}\left(\begin{pmatrix} \hat{\mu}_{ij} \\ \hat{\mu}_{ik} \end{pmatrix}, \begin{pmatrix} 1 & \rho_{jk} \\ \rho_{jk} & 1 \end{pmatrix}\right).$$

The model-implied joint success probability for item i is

$$p_{11}^{(i)}(j, k; \rho_{jk}) := \mathbb{P}(Y_{ij} = 1, Y_{ik} = 1) = \Phi_2(\hat{\mu}_{ij}, \hat{\mu}_{ik}; \rho_{jk}),$$

where $\Phi_2(\cdot, \cdot; \rho)$ is the bivariate normal CDF with correlation ρ . The model-implied covariance between $Y_{\cdot j}$ and $Y_{\cdot k}$ is

$$C_{jk}^{\text{model}}(V) = \frac{1}{N} \sum_{i=1}^N p_{11}^{(i)}(j, k; \rho_{jk}) - \hat{m}_j \hat{m}_k, \quad \rho_{jk} = v_j^\top v_k. \quad (6)$$

The empirical covariance is

$$C_{jk}^{\text{emp}} = \frac{1}{N} \sum_{i=1}^N Y_{ij} Y_{ik} - \bar{Y}_j \bar{Y}_k. \quad (7)$$

For each iteration, the implementation computes these quantities in a streaming/tiled fashion over items and model blocks, but conceptually they are just (6)–(7).

Loss and gradients in correlation space. We fit V by matching model-implied and empirical covariances off the diagonal. The loss is

$$\mathcal{L}(V) = \sum_{1 \leq j < k \leq M} (C_{jk}^{\text{model}}(V) - C_{jk}^{\text{emp}})^2. \quad (8)$$

To differentiate with respect to ρ_{jk} , note that

$$\frac{\partial}{\partial \rho_{jk}} p_{11}^{(i)}(j, k; \rho_{jk}) = \varphi_2(\hat{\mu}_{ij}, \hat{\mu}_{ik}; \rho_{jk}),$$

where φ_2 is the bivariate normal PDF with correlation ρ_{jk} . Hence

$$\frac{\partial C_{jk}^{\text{model}}}{\partial \rho_{jk}} = \frac{1}{N} \sum_{i=1}^N \varphi_2(\hat{\mu}_{ij}, \hat{\mu}_{ik}; \rho_{jk}) =: \bar{\varphi}_{jk},$$

and by the chain rule,

$$\frac{\partial \mathcal{L}}{\partial \rho_{jk}} = 2(C_{jk}^{\text{model}} - C_{jk}^{\text{emp}}) \bar{\varphi}_{jk}. \quad (9)$$

In the code, $C_{jk}^{\text{model}} - C_{jk}^{\text{emp}}$ is stored as `diff_blk`, and $\bar{\varphi}_{jk}$ as `phibar_blk`, so that

$$G_{jk} := \frac{\partial \mathcal{L}}{\partial \rho_{jk}} = 2 \text{diff_blk}_{jk} \text{phibar_blk}_{jk}.$$

Gradients in embedding space and optimization. Because $\rho_{jk} = v_j^\top v_k$ for $j \neq k$, we have

$$\frac{\partial \rho_{jk}}{\partial v_j} = v_k, \quad \frac{\partial \rho_{jk}}{\partial v_k} = v_j,$$

and thus

$$\frac{\partial \mathcal{L}}{\partial v_j} = \sum_{k \neq j} \frac{\partial \mathcal{L}}{\partial \rho_{jk}} \frac{\partial \rho_{jk}}{\partial v_j} = \sum_{k \neq j} G_{jk} v_k. \quad (10)$$

In matrix form, if G is the matrix with entries G_{jk} (symmetric and zero on the diagonal), then the gradient w.r.t. V is

$$\nabla_V \mathcal{L} = GV,$$

which is exactly what the code accumulates in the tensor Z . We then perform Adam updates on V :

$$V \leftarrow \text{AdamStep}(V, \nabla_V \mathcal{L}),$$

with bias-corrected learning rate as in standard Adam.

Norm projection and unit variance. After each Adam update, we project each row v_j onto the unit ball:

$$v_j \leftarrow \frac{v_j}{\max\{1, \|v_j\|_2\}}. \quad (11)$$

This ensures $\|v_j\|_2 \leq 1$ for all j , so that the covariance matrix Σ in (5) remains positive semidefinite with unit diagonal. Conceptually, we are learning a low-rank correlation structure $\rho_{jk} = v_j^\top v_k$ subject to the constraint that all variances are fixed at one, which preserves the scaling of the underlying 1D IRT model.

Practical details. The implementation evaluates the loss (8) and its gradients exactly but does so in a memory-efficient way by: (i) streaming over items in chunks (size `item_chunk`) and (ii) tiling the model index set into blocks (size `model_block`) to compute C_{jk}^{model} and C_{jk}^{emp} blockwise. We use early stopping based on the best observed loss over iterations.

Justification for two-stage estimation. This two-stage procedure separates *first-order* and *second-order* structure: Stage 1 uses only the marginal success probabilities to learn (θ, b) , while Stage 2 uses the residual covariances to learn Σ . Under standard regularity conditions, the Stage 1 maximum-likelihood estimates $(\hat{\theta}, \hat{b})$ are consistent and \sqrt{N} -accurate even if $\Sigma \neq I_M$, because the marginal Bernoulli probabilities depend only on (θ, b) and not on Σ . Plugging these into the second-stage moment-matching objective yields a consistent estimator of Σ that is asymptotically equivalent to a joint estimator but computationally simpler. Conceptually, this is analogous to generalized method-of-moments procedures that estimate parameters associated with lower-order moments before fitting higher-order structure.